Grid Topology Identification via Distributed Statistical Hypothesis Testing

Saverio Bolognani
Automatic Control Laboratory
ETH Zürich

Section Three: Put the Power of Big Data into Power Systems
Keywords: grid topology, distribution networks, graphical models.

Abstract

We consider the problem of automatically identifying the topology of a power distribution network, based on data measurements collected on the grid. Possible applications include the detection of changes in the operational topology, the deployment and tuning of plug-and-play volt-VAR regulators, and the implementation of active management strategies for congestion relief.

We first show, by using a first-order model of the grid, that voltage measurements exhibit some specific correlation properties, that can be described via a sparse Markov random field. By specializing the tools available for the identification of graphical models, we propose a centralized algorithm for the reconstruction of the grid topology.

We then show how it is possible to formulate the grid topology identification task as a series of distributed statistical tests that agents need to perform on their measurements. As the number of collected samples increases, agents can answer the test with increasing confidence, select the correct hypothesis (e.g. a switch being open or close), and ultimately infer the grid topology. The computational complexity of each of these tests is independent from the grid size.

The effectiveness of both the centralized and the distributed approach are tested in simulations, based on household power demand measurements from a real distribution feeder.

1 Introduction

Power distribution networks, compared to transmission systems, have been historically planned and designed according to a *fit-and-forget* approach. During operation, these grids remain mostly unmonitored, with minimal sensing and actuation, and often no communication infrastructure available to collect measurements or dispatch real time commands.

Different challenges are now emerging in the power distribution network, and are motivating a much deeper integration of information, communication, and control technology in this realm. One example is the large-scale penetration of microgenerators from fluctuating energy sources. Distributed power generation, especially inside the highly resistive, radial, low voltage networks, can cause local overvoltage and power line congestions issues [1]. Another example is the connection of dispatchable loads to the power distribution network, e.g. plugin electric vehicles and smart buildings. Today's power distribution grid will face major congestion issues if proper scheduling and coordination protocols will not be enforced to these consumers [2, 3].

In the last few years, international research projects have been funded in order to develop and engineer solutions to these challenges, while maintaining grid efficiency and reliability [4, 5, 6, 7]. Many of these solutions require that the topology of the power distribution grid is known, which is not always true. In many cases, the deployment of intelligence in the power distribution grid will consist of retro-fitting an existing infrastructure via the installation of new devices. A *plug-and-play* approach is often considered and may constitute in some cases the only viable solution. According to this approach, the devices must identify the physical system in which they operate, starting

from the topology of the grid, and reconfigure the communication and control infrastructure in order to being able to perform the assigned tasks. Even after deployment, the topology of the grid may be subject to changes, via the operation of dedicated switches to achieve higher efficiency or better quality of the service. Such changes of topology need to be detected by the controllers in the grid, which in turn need to be promptly reconfigured.

In this chapter, we consider the problem of identifying the grid topology from field measurements that can be performed in the grid, and in particular from voltage magnitude measurements at the buses. The approach proposed in this paper is closely related to the methods for the identification of Markov random fields (graphical models) [8], and is based on some conditional correlation properties that characterize voltage measurements in a radial grid. These properties are reported in Section 3, where they are also used to derive a centralized topology identification algorithm. In Section 4, we show how the same reasoning can be used to design distributed tests that involve only three nodes, and return elementary bits of information regarding the topology of the grid. These tests require minimal sensing and computational resources, and return a reliable response after an extremely limited number of measurement samples. Both the correlation analysis and the distributed identification algorithms are tested in Section 5 on power measurements data obtained from a real distribution network.

Related works

The literature on grid topology identification is mostly divided into two areas: works that consider the problem of determining the position of a limited number of grid switches, and therefore test a limited number of hypotheses, and works that aim at identifying the entire topology of a feeder. We review these two areas separately in the next two paragraphs.

The idea of using field measurements to detection of unmonitored switching of circuit breakers in the reconfiguration of the power distribution grid has been presented for example in [9], where the task has been formulated as a classification problem. More recently, correlation analysis methods have been proposed to verify whether the topology available in a geographic information system is correct [10], tackling the problem as a hypothesis testing problem. An algorithm for real time detection of topology changes, based on PMU measurements and on the identification of patterns in the time series following a switching event, has been proposed in [11]. The Markov-random-field nature of voltage phasor measurements have been recognized in [12], and used as a test for fault detection.

Algorithm like the one proposed in [13], on the other hand, aim at reconstructing the entire topology, without assuming any specific library of possible configurations. The mathematical analysis presented in this chapter is adopted (and extended) from there. More recently, the same idea of constructing a minimum-cost spanning tree for the identification of the power distribution network, which is closely related to the Chow-Liu algorithm for graphical models, have been used in [14] on the mutual information matrix, yielding better performance but still requiring very large number of samples. Topology learning tools based on the trends in second order moments of voltage measurements have been proposed in [15, 16]. Interestingly, the same authors also considered the case in which some measurements are missing, a challenging problem in graphical learning [17]. In [18], the bus connectivity and topology estimation problems are formulated as a linear regression problem with least absolute shrinkage on grouped variables (Group Lasso).

In all these works synthetic data are used rather than real measurements. A notable exception is [19], where however linear voltage sensitivity coefficients are computed, without enforcing sparsity or tree structure.

2 Power distribution grid model

We model a power distribution grid as a radial graph $\mathcal{G}$, in which edges represent the power lines, and nodes $\mathcal{V} = \{0, \dots, n\}$ represent the buses of the grid (including the substation, indexed as 0).

We limit the study to a grid-connected distribution feeder, and we therefore assume that the voltage at node 0 is constant (i.e., it does not depend on the power demands in the feeder), and that all other nodes $h \in \mathcal{L} := \{1, \dots, n\}$ can be modeled as PQ buses (i.e., with an active and reactive power demand that does not depend on the bus voltage).

In this framework, the steady state of the grid is described by the following nodal quantities, for each node $h \in \mathcal{V}$:

- complex voltage $u_h = v_h e^{j\theta_h}$
- complex power injection $s_h = p_h + jq_h$
- complex current injection i_h

Based on this notation, we write the nonlinear power flow equations of the grid as $n+1$ complex-valued equations of the form

$$v_h e^{j\theta_h} \sum_{k \in \mathcal{V}} \bar{y}_{hk} v_k e^{-j\theta_k} = p_h + jq_h, \quad \forall h \in \mathcal{V}, \tag{1}$$

where $\bar{y}_{hk}$ is the complex conjugate of the admittance of the line connecting h to k, and $y_{hh} = -\sum_{k \neq h} y_{hk}$ (assuming negligible shunt admittances at the buses).

For the subsequent analysis, it is convenient to introduce the following vectorial notation. We denote by v, s, p, q the vectors of dimension n, obtained by stacking the scalar quantities v_h, s_h, p_h, q_h, respectively, for all $h \in \mathcal{L}$. Similarly, we partition the bus admittance matrix Y, whose elements are the scalars y_{hk}, as

$$Y = \begin{bmatrix} Y_{00} & Y_{0\mathcal{L}} \\ Y_{\mathcal{L}0} & Y_{\mathcal{L}\mathcal{L}} \end{bmatrix}$$

where $Y_{\mathcal{L}\mathcal{L}}$ has dimensions $n \times n$.

For the subsequent analysis, we consider the linearization of the nonlinear power flow equations (1) around the flat voltage profile ($v_h = v_0, \forall h \in \mathcal{V}$), corresponding to the *Linear Coupled power flow model*. We refer to [20, Section V] for the derivation of the model, and to [21] for a geometric interpretation of this linearization. Based on this approximation, voltage magnitudes at the buses in $\mathcal{L}$ can be expressed as

$$v \approx \mathbf{1} v_0 + \frac{1}{v_0} \operatorname{Re}(Z\bar{s}) \tag{2}$$

where the bus impedance matrix $Z \in \mathbb{C}^{n \times n}$ is defined as $Z = Y_{\mathcal{L}\mathcal{L}}^{-1}$.

We recall that the elements of the bus impedance matrix have the following well known interpretation in the case of radial networks.

Definition (Shortest electric path)**.** Given two buses $h, k \in \mathcal{V}$, we define the electric path $\mathcal{P}_{hk}$ as the smallest connected subset of nodes of $\mathcal{V}$ such that $h, k \in \mathcal{P}_{hk}$.

Lemma 1. *Let h, k be two buses in $\mathcal{V}$, and let $\mathcal{P}_{0h}$ and $\mathcal{P}_{0k}$ be the shortest electric paths that connect them to node 0. Then Z_{hk} is the sum of the impedances of the edges connecting the nodes in the intersection $\mathcal{P}_{0h} \cap \mathcal{P}_{0k}$.*

Without loss of generality, in the following, we assume $v_0 = 1$. We also consider the approximation error in (2) negligible, and therefore adopt the grid model

$$v = \mathbf{1} + Rp + Xq, \tag{3}$$

where $R = \operatorname{Re}(Z)$ and $X = \operatorname{Im}(Z)$ are the reduced bus resistance and reactance matrices, respectively.

3 Voltage correlation analysis

In this section, we review and extend the voltage correlation analysis proposed for the first time in [13], as it lays the groundwork for the derivation of the proposed distributed identification strategy.

Based on (3), the covariance matrix of the bus voltages can be directly expressed as

$$\begin{aligned} \operatorname{cov}(v) &= \mathbb{E}\,(v - \mathbb{E}\,v)\,(v - \mathbb{E}\,v)^T \\ &= \mathbb{E}\,(R(p - \mathbb{E}\,p) + X(q - \mathbb{E}\,q))\,(R(p - \mathbb{E}\,p) + X(q - \mathbb{E}\,q))^T \\ &= R\Sigma_{pp}R + X\Sigma_{qp}R + R\Sigma_{pq}X + X\Sigma_{qq}X \end{aligned} \tag{4}$$

where

$$\begin{bmatrix} \Sigma_{pp} & \Sigma_{pq} \\ \Sigma_{qp} & \Sigma_{qq} \end{bmatrix}$$

is the positive definite covariance matrix of the bus power injection vector $[p^T q^T]^T$.

The covariance matrix (4) clearly contains information regarding the topology of the grid, which is encoded in the matrices R and X. For this information to be reconstructable, we need the following assumption.

Assumption 1 (Uncorrelated power demands)**.** *Active and reactive power injections at different buses are mutually uncorrelated. Therefore $\Sigma_{pp}, \Sigma_{pq}, \Sigma_{qp}$, and Σ_{qq} are all diagonal matrices.*

Assumption 1 is a critical step in the derivation of correlation-based topology identification methods, and has been adopted throughout the literature reviewed in the Introduction. In Section 5 we verify whether this assumption holds on the power measurements from a real distribution feeder, and we discuss how it depends on the time scale under consideration.

We then introduce two other assumptions that will be later employed in the analysis.

Assumption 2 (Uniform X/R ratio)**.** *All power lines in the distribution grid have the same inductance/resistance ratio, i.e.*

$$y_{hk} = e^{j\theta}|y_{hk}|, \qquad \forall h, k \in \mathcal{V},$$

where θ is fixed across the network.

Assumption 2 is satisfied when the grid is relatively homogeneous, and is reasonable in most practical cases, including the IEEE test feeder considered in the numerical experiments of Section 5.

Assumption 3 (Uniform power factor)**.** *All loads in the distribution feeder have the same power factor, i.e.*

$$q_h = \kappa p_h, \qquad \forall h \in \mathcal{L},$$

where κ is fixed across the network.

Notice that Assumption 3 is trivially verified if the loads are perfectly compensated, in which case $\kappa = 0$ and thus $q_h = 0$ for all $h \in \mathcal{L}$.

We can therefore state the following result, which shows how it is possible to compute the voltage covariance matrix a completely equivalent purely resistive grid.

Lemma 2 (Equivalent resistive grid)**.** *Let Assumption 1 hold, together with either Assumption 2 or Assumption 3. Then there exists a purely resistive network, with the same topology of $\mathcal{G}$, bus conductance matrix G, and uncorrelated active power injections with covariance matrix Σ, which yields the same voltage covariance matrix $\mathrm{cov}(v)$ as the original grid.*

Moreover, the voltage covariance matrix can be explicitly expressed as

$$\mathrm{cov}(v) = M\Sigma M$$

where $M = G^{-1}_{\mathcal{L}\mathcal{L}}$.

Proof. Let us first consider the case in which Assumption 2 holds. Then $Y = e^{j\theta}Y'$, where $Y' \in \mathbb{R}^{(n+1)\times(n+1)}$. It follows that $R = \mathrm{Re}\left(Y^{-1}_{\mathcal{L}\mathcal{L}}\right) = \cos\theta\,(Y'_{\mathcal{L}\mathcal{L}})^{-1}$ and $X = \mathrm{Im}\left(Y^{-1}_{\mathcal{L}\mathcal{L}}\right) = -\sin\theta\,(Y'_{\mathcal{L}\mathcal{L}})^{-1}$. Therefore $X = -\tan\theta R$, and expression (4) can be rewritten as

$$\mathrm{cov}(v) = R\left(\Sigma_{pp} - 2\tan\theta\Sigma_{qp} + \tan^2\theta\Sigma_{qq}\right)R.$$

The statement of the lemma is therefore verified by defining the positive definite matrix

$$\Sigma = \Sigma_{pp} - 2\tan\theta\Sigma_{qp} + \tan^2\theta\Sigma_{qq} = \begin{bmatrix} I & -\tan\theta I \end{bmatrix} \begin{bmatrix} \Sigma_{pp} & \Sigma_{pq} \\ \Sigma_{qp} & \Sigma_{qq} \end{bmatrix} \begin{bmatrix} I \\ -\tan\theta I \end{bmatrix}$$

and by considering the graph Laplacian $G = \mathrm{Re}(Y)$.

Let us now consider the case in which Assumption 3 holds. Then $\Sigma_{pq} = \Sigma_{qp} = \kappa\Sigma_{pp}$ and $\Sigma_{qq} = \kappa^2\Sigma_{pp}$. Expression (4) can be manipulated to obtain

$$\mathrm{cov}(v) = (R + \kappa X)\Sigma_{pp}(R + \kappa X).$$

The statement of the lemma is therefore verified by taking $\Sigma = \Sigma_{pp}$ (which is positive definite) and by considering the graph Laplacian G obtained by weighting each edge hk as $\mathrm{Re}(y_{hk}) - \kappa\,\mathrm{Im}(y_{hk})$, where y_{hk} is the admittance of the corresponding power line. □

Lemma 2 is instrumental to prove the following result, which shows how the inverse of the covariance matrix $\mathrm{cov}(v)$ is sparse and has a specific sign pattern.

Theorem 1. *Let Assumption 1 hold, together with either Assumption 2 or Assumption 3. Let $K = \mathrm{cov}(v)^{-1}$. Then for any pair h, k in $\mathcal{L}$ we have that*

$$K_{hk} \begin{cases} > 0 & \text{if } h = k \\ < 0 & \text{if } h \sim k \\ > 0 & \text{if } \exists \ell \in \mathcal{L} \text{ such that } h \sim \ell \text{ and } \ell \sim k \\ 0 & \text{otherwise,} \end{cases}$$

where the $\sim$ sign indicates neighbors in the electric topology (i.e., there exists an edge of the graph connecting them).

Proof. Based on Lemma 2, the matrix K can be explicitly expressed as

$$K = \mathrm{cov}(v)^{-1} = (M\Sigma M)^{-1} = G_{\mathcal{L}\mathcal{L}}\Sigma^{-1}G_{\mathcal{L}\mathcal{L}}$$

for some positively-weighted Laplacian L and some positive definite diagonal matrix Σ^{-1}. We introduce the notation

$$\Sigma^\dagger = \begin{bmatrix} 0 & 0 \\ 0 & \Sigma^{-1} \end{bmatrix} \in \mathbb{R}^{(n+1)\times(n+1)}.$$

By defining $\mathcal{N}(h)$ as the set of neighbors of node h, and by using the fact that G is a positively-weighted Laplacian and therefore

$$G_{hk} \begin{cases} > 0 & \text{if } h = k \\ < 0 & \text{if } h \sim k \\ 0 & \text{otherwise,} \end{cases}$$

we have that

$$\mathbf{1}_h^T G\Sigma^\dagger G\mathbf{1}_k = \left(G_{hh}\mathbf{1}_h^T + \sum_{h' \in \mathcal{N}(h)} G_{hh'}\mathbf{1}_{h'} \right) \Sigma^\dagger \left(\mathbf{1}_k G_{kk} + \sum_{k' \in \mathcal{N}(k)} \mathbf{1}_{k'} G_{k'k} \right).$$

Now, using the fact that

$$\mathbf{1}_v^T \Sigma^\dagger \mathbf{1}_w = \begin{cases} (\Sigma_{vv})^{-1} > 0 & \text{if } v = w \neq 0 \\ 0 & \text{otherwise,} \end{cases}$$

we have that, in $\mathcal{L}$,

- for all h,

$$K_{hh} = \mathbf{1}_h^T G\Sigma^\dagger G\mathbf{1}_h = G_{hh}\left(\Sigma_{hh}\right)^{-1} G_{hh} + \sum_{\ell \in \mathcal{N}(h)} G_{h\ell}\left(\Sigma_{\ell\ell}\right)^{-1} G_{\ell h} > 0;$$

- if $h \sim k$ then

$$K_{hk} = \mathbf{1}_h^T G\Sigma^\dagger G\mathbf{1}_k = G_{hh}\left(\Sigma_{hh}\right)^{-1} G_{hk} + G_{hk}\left(\Sigma_{kk}\right)^{-1} G_{kk} < 0;$$

- if $h \neq k$ and $\exists \ell$ such that $\ell \sim h$ and $\ell \sim k$, then

$$K_{hk} = \mathbf{1}_h^T G\Sigma^\dagger G\mathbf{1}_k = G_{h\ell}\left(\Sigma_{\ell\ell}\right)^{-1} G_{\ell k} > 0;$$

- $K_{hk} = \mathbf{1}_h^T G\Sigma^\dagger G\mathbf{1}_k = 0$ otherwise.

□

Remark. The matrix K is known as *concentration matrix*, and has an interesting and well known interpretation in terms of conditional correlation. In particular, $K_{hk} = 0$ if and only if v_h and v_k are conditionally uncorrelated given all other voltages v_ℓ, $\ell \neq h, k$. According to Theorem 1, the sparsity pattern of K is the same of $Y^2_{\mathcal{L}\mathcal{L}}$. In the terminology of Markov random fields [8], this means that the corresponding graphical model is an undirected graph in which nodes are connected by an edge (and therefore are conditionally correlated) if they are 1-hop or 2-hop neighbors in the graph describing the power distribution grid topology.

Theorem 1 also shows that the strictly negative elements of K have the sparsity pattern of $Y_{\mathcal{L}\mathcal{L}}$ and can therefore be directly used to reconstruct the electrical topology of the grid.

Based on these observations, we propose the following steps for the identification of the grid topology, given a sequence of T voltage measurements at all buses of the grid, $v^{(t)}$, $t = 1, \dots, T$.

1. Compute the sample covariance matrix $\hat{\Sigma} = \mathrm{cov}(v^{(t)}, t = 1, \dots, T)$.
2. Compute the sample concentration matrix $\hat{K}$ as $\hat{\Sigma}^{-1}$.
3. Consider the complete graph $\mathcal{C}$ defined on the nodes $\mathcal{L}$, with edge weights corresponding to the elements of $\hat{K}$. Compute the *minimum spanning tree* on $\mathcal{C}$, i.e. the subgraph of $\mathcal{C}$ that is a tree, connects all the nodes, and whose total edge cost is less or equal to any other spanning tree.

Notice that the minimum spanning tree can be computed in polynomial time by greedy algorithms like the Prim's algorithm [22].

The proposed algorithm resembles, in some sense, the well known Chow-Liu algorithm [23] for graphical model identification, in which however the choice of the best spanning tree is motivated by the search for the closest approximation of the actual distribution in an information-theoretic sense. In our scenario, on the other hand, we know in advance that there exists a tree which is the *root* (in the graph-theory sense) of the graph that describes the actual distribution (i.e. the actual graph connects nodes that can be reached in 1 or 2 hops in such tree), and we make explicit use of this additional information. Because of this *a priori* knowledge, we also don't need the tools that have been developed for model selection [24] (i.e., to tune the sparsity of the estimated graph).

In Section 5 we illustrate the voltage correlation analysis presented in this section, by considering a dataset of real power demand measurements and by implementing the proposed identification algorithm. We show how this algorithm typically requires a large number of samples, and how its performance deteriorates when the assumptions are not verified.

4 A distributed topology test

As reviewed in the Introduction, different approaches based on similar statistical analysis of voltage measurements have been proposed, improving the topology detection rate and in some cases reducing the number of samples needed [15, 16, 14]. These works, however, consider the same centralized scenario introduced in Section 3. Voltages at all nodes are supposed to be measured (with the possible exception of few nodes, as suggested in [17]), making the implementation of these schemes impractical in poorly monitored networks.

In this section, the same correlation-based approach will be employed to derive a set of distributed topology tests, where small clusters of three buses will have to communicate and share their voltage measurements in order to provide elementary bits of information regarding the topology of the grid. This approach better suits the typical needs of distribution network operators: it requires a minimal amount of sensing (three bus voltage sensors) and it allows to discern simple (but relevant) hypotheses on the grid topology, such as

- whether a switch is open or closed
- which of the three sensor lies closest to the substation, in an electrical sense
- what is the relative position of a newly connected sensor with respect to other sensors.

In order to present the details of this approach, we introduce the following definitions, which are also illustrated in Figure 1 and apply only to radial graphs.

Definition (Triad)**.** A set of three buses $\mathcal{T} \subset \mathcal{L}$ is a triad, if one of the three buses belongs to the shortest electric path that connects the other two.

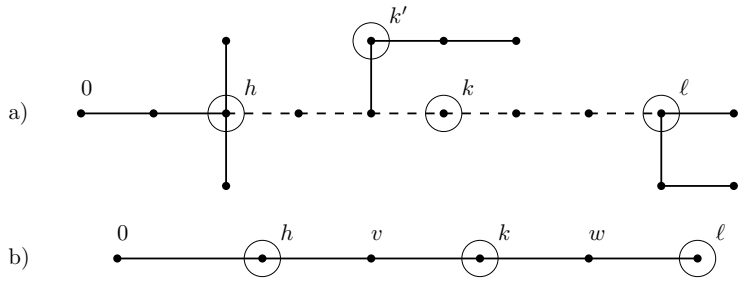

Figure 1: Schematic representation of the definitions introduces in Section 4. a) The subset of buses $\mathcal{T} = \{h, k, \ell\}$ is a *triad* because k belongs to the *shortest electric path* $\mathcal{P}_{h\ell}$ (the thick dashed path). The subset $\{h, k', \ell\}$ is not a triad. b) The *minimal interleaved graph* that connects the triad $\mathcal{T}$.

Definition (Minimal interleaved graph)**.** A graph is a minimal interleaved graph connecting a triad $\mathcal{T}$ if it is obtained by interleaving $\mathcal{T}$ with another triad $\mathcal{T}' = \{0, v, w\}$, as shown in Figure 1.

Definition (Node depth)**.** Given a bus $h \in \mathcal{V}$, and a weighted Laplacian G, we define the node depth x_h as the sum of the weights of the edges that connect the nodes in the shortest electric path $\mathcal{P}_{0h}$.

Based on these definitions, we can state the following result, which shows that the voltage covariance at the buses of a triad is identical to the voltage covariance of a triad in a much smaller purely resistive grid, with properly chosen line parameters and active power injection covariance.

Lemma 3 (Minimal equivalent resistive grid)**.** *Let Assumption 1 hold, together with either Assumption 2 or Assumption 3. Consider a triad $\mathcal{T} = \{h, k, \ell\}$. Then there exists a minimal equivalent resistive grid, whose graph is a minimal interleaved graph connecting $\mathcal{T}$, with conductance matrix $\tilde{G}$ and diagonal power covariance $\tilde{\Sigma}$, which yields the same covariance* $\mathrm{cov}(v_{\mathcal{T}})$ *of the voltages at the nodes h, k, ℓ.*

Proof. The proof is constructive, and follows these steps, which are also depicted in Figure 2.

- Based on Lemma 2, we consider the equivalent resistive grid with positively-weighted Laplacian G and power covariance Σ (step a).
- Without loss of generality, we lump all the power demands in each *lateral* (i.e., branches that do not belong to the path $\mathcal{P}_{0\ell}$) to the node where the lateral connects (step b).
- We denote by $\mathcal{L}_1$, $\mathcal{L}_2$, and $\mathcal{L}_3$, the three subsets of nodes indicated in step b.
- We consider the minimal interleaved graph in step c, with positively weighted Laplacian $\tilde{G}$ such that nodes h, k, ℓ have the same depths x_h, x_k, x_ℓ as in the original graph with Laplacian G, while nodes v and w have depths

$$x_v = \frac{\sum_{i\in\mathcal{L}_2} x_i\sigma_i(x_i - x_h)}{\sum_{i\in\mathcal{L}_2} \sigma_i(x_i - x_h)}$$
$$x_w = \frac{\sum_{i\in\mathcal{L}_3} x_i\sigma_i(x_i - x_k)}{\sum_{i\in\mathcal{L}_3} \sigma_i(x_i - x_k)}$$

  where σ_i is the diagonal element of Σ corresponding to node i.

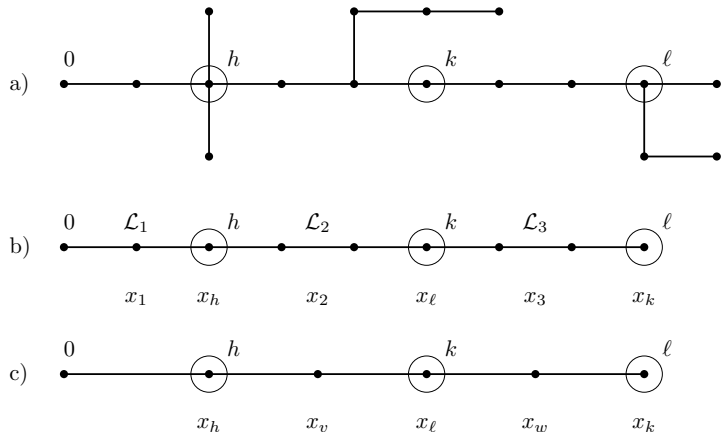

Figure 2: Schematic representation of the steps of the constructive proof of Lemma 3.

- We construct the diagonal power covariance matrix $\tilde{\Sigma}$ with diagonal elements

$$\begin{aligned}
\tilde{\sigma}_v &= \frac{\sum_{i\in\mathcal{L}_2}\sigma_i(x_i - x_h)}{x_v - x_h} \\
\tilde{\sigma}_w &= \frac{\sum_{i\in\mathcal{L}_3}\sigma_i(x_i - x_k)}{x_w - x_k} \\
\tilde{\sigma}_h &= \sigma_h + \frac{\sum_{i\in\mathcal{L}_1} x_i^2\sigma_i}{x_h^2} + \sum_{i\in\mathcal{L}_2}\sigma_i - \tilde{\sigma}_v \\
\tilde{\sigma}_k &= \sigma_k + \sum_{i\in\mathcal{L}_3}\sigma_i - \tilde{\sigma}_w \\
\tilde{\sigma}_\ell &= \sigma_\ell.
\end{aligned}$$

The voltage covariance matrix for the minimal equivalent resistive grid can be computed as $\tilde{M}\tilde{\Sigma}\tilde{M}$. Using the fact that, for line graphs, $M_{ij} = \min\{x_i, x_k\}$ (which follows directly from Lemma 1), via lengthy but otherwise standard computations, it is possible to show that the covariance of the triad voltages $v_\mathcal{T}$ is the same in the original equivalent resistive grid and in the minimal equivalent resistive grid. Via Lemma 2, the same covariance matrix is also equal to the voltage covariance $\mathrm{cov}(v_\mathcal{T})$ in the original grid. □

The purpose of the equivalence introduced by Lemma 3 is to allow a much simpler study of the voltage covariance matrix $\mathrm{cov}(v_\mathcal{T})$. In fact, for a minimal interleaved graph, it is possible to explicitly write $\mathrm{cov}(v_\mathcal{T})$ as a function of the parameters $\tilde{G}$ and $\tilde{\Sigma}$. This fact is used to obtain the following result.

Theorem 2. *Let Assumption 1 hold, together with either Assumption 2 or Assumption 3.*

Consider a triad $\mathcal{T} = \{h, k, \ell\}$, in which $k \in \mathcal{P}_{h\ell}$, and let $\mathrm{cov}(v_\mathcal{T})$ be the covariance of the voltages at the buses h, k, ℓ. Then the matrix $K = [\mathrm{cov}(v_\mathcal{T})]^{-1}$ has sign pattern

$$sign(K) = \begin{bmatrix} +1 & -1 & +1 \\ -1 & +1 & -1 \\ +1 & -1 & +1 \end{bmatrix}.$$

Proof. We first construct, via Lemma 2, an equivalent resistive network. Then, via Lemma 3, we consider a minimal equivalent resistive network which is guaranteed to yield the same voltage covariance matrix at the nodes of the triad.

The voltage covariance matrix $\mathrm{cov}(v_{\mathcal{T}})$ can be then obtained by selecting the rows and columns of the full voltage covariance matrix $\mathrm{cov}(v) = \tilde{M}\tilde{\Sigma}\tilde{M}$. Using Lemma 1, we can write

$$\mathrm{cov}(v_{\mathcal{T}}) = N \begin{bmatrix} \tilde{\sigma}_h & & & & \\ & \tilde{\sigma}_v & & & \\ & & \tilde{\sigma}_k & & \\ & & & \tilde{\sigma}_w & \\ & & & & \tilde{\sigma}_\ell \end{bmatrix} N^T \quad \text{where} \quad N = \begin{bmatrix} \tilde{x}_h & \tilde{x}_h & \tilde{x}_h & \tilde{x}_h & \tilde{x}_h \\ \tilde{x}_h & \tilde{x}_v & \tilde{x}_k & \tilde{x}_k & \tilde{x}_h \\ \tilde{x}_h & \tilde{x}_v & \tilde{x}_k & \tilde{x}_w & \tilde{x}_\ell \end{bmatrix}$$

As the determinant of K is positive, the sign pattern of K is the same sign pattern of $\mathrm{adjoint}(\mathrm{cov}(v_{\mathcal{T}}))$. The matrix $\mathrm{adjoint}(\mathrm{cov}(v_{\mathcal{T}}))$ can be evaluated via standard symbolic math software. It is convenient to operate a change of variable, introducing the positive depth differences $\delta_{h0} = \tilde{x}_h$, $\delta_{vh} = \tilde{x}_v - \tilde{x}_h$, $\delta_{kv} = \tilde{x}_k - \tilde{x}_v$, $\delta_{wk} = \tilde{x}_w - \tilde{x}_k$, and $\delta_{\ell w} = \tilde{x}_\ell - \tilde{x}_w$. The elements of $\mathrm{adjoint}(\mathrm{cov}(v_{\mathcal{T}}))$ are fourth-order polynomials in these quantities. For example, we have that

$$[\mathrm{adjoint}(\mathrm{cov}(v_{\mathcal{T}}))]_{\ell\ell} =$$
$$\tilde{\sigma}_h(\tilde{\sigma}_k + \tilde{\sigma}_\ell + \tilde{\sigma}_v + \tilde{\sigma}_w)\delta_{h0}^2\delta_{vh}^2 + 2\tilde{\sigma}_h(\tilde{\sigma}_k + \tilde{\sigma}_\ell + \tilde{\sigma}_w)\delta_{h0}^2\delta_{vh}\delta_{kv} + (\tilde{\sigma}_h + \tilde{\sigma}_v)(\tilde{\sigma}_k + \tilde{\sigma}_\ell + \tilde{\sigma}_w)\delta_{h0}^2\delta_{kv}^2$$

We do not report here for space reasons. The sign of all the elements of $\mathrm{adjoint}(\mathrm{cov}(v_{\mathcal{T}}))$ is then apparent by inspection, and the matrix K exhibits the sign pattern

$$\mathrm{sign}(K) = \begin{bmatrix} +1 & -1 & +1 \\ -1 & +1 & -1 \\ +1 & -1 & +1 \end{bmatrix}.$$

□

Based on Theorem 2, we can then propose the following steps as a distributed hypothesis test. Given a triad $\mathcal{T}$, and a sequence of T voltage measurements at the three buses in $\mathcal{T}$, $v_{\mathcal{T}}^{(t)}$, $t = 1, \ldots, T$, this test determines which node of the triad belongs to the shortest electric path that connects the other two nodes (in other words, the "order" of the nodes in the triad). It consists of the following steps.

1. Compute the 3×3 sample covariance matrix $\hat{\Sigma}_{\mathcal{T}} = \mathrm{cov}(v_{\mathcal{T}}^{(t)}, t = 1, \ldots, T)$.
2. Compute the 3×3 sample concentration matrix $\hat{K}$ as $\hat{\Sigma}_{\mathcal{T}}^{-1}$.
3. Consider the complete graph $\mathcal{C}$ defined on the nodes $\mathcal{T}$, with edge weights corresponding to the elements of $\hat{K}$. Compute the *minimum spanning tree* on $\mathcal{C}$, i.e. the line subgraph of $\mathcal{C}$ that connects the three nodes, and whose total edge cost is less or equal to any other spanning tree.

The advantage of this approach is that the test has to identify the most likely topology among only three possible topologies of the triad, resulting in a much smaller search space. For example, in the scenario represented in Figure 3, a distribution grid operator may be interested in knowing whether switch S1 or S2 is closed. By selecting the triad $\{h, k, \ell\}$, this binary question is cast into the form of a hypothesis test on the relative topology of the nodes in the triad: if $k \in \mathcal{P}_{h\ell}$, then S1 must be open while S2 must be closed; on the other hand, if $h \in \mathcal{P}_{k\ell}$, then S2 must be open, and S1 must be closed. We show in Section 5 that very few samples are needed in order to identify the correct hypothesis in similar configurations.

5 Numerical experiments

In this section, we use a dataset of power demand measurements from a real power distribution grid to validate both the correlation analysis presented in Section 3 and the distributed algorithm proposed in Section 4.

The dataset is provided as part of the DiSC simulation framework [25], and has been obtained as anonymized data from the Danish DSO NRGi. It represents the power consumption of about 1200 individual households from the area around the Danish city Horsens. Each profile has a temporal resolution of 15 minutes, and spans more than a year. In order to recreate the sub-15

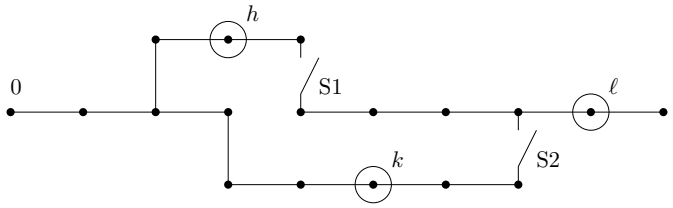

Figure 3: An example of how the problem of determining the position of a pair of grid switches can be cast into the problem of determining the relative position of the nodes of a triad $\{h, k, \ell\}$.

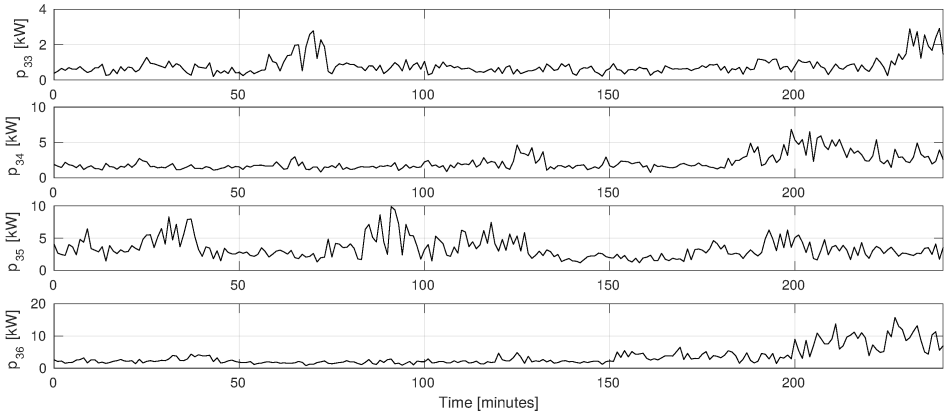

Figure 4: Example of demand profiles for four buses of the test case. Each bus demand is obtained as the aggregation of multiple real data measurements from individual buildings.

minute variability of loads, we superimposed power demand fluctuations obtained via a simple generative model similar to the one proposed in [26].

As a test feeder, we adopted the test feeder proposed in [20], available as an online repository [27], and consisting in the three-phase backbone of the standard IEEE 123 distribution test feeder [28]. At each bus of the feeder, we considered an aggregation of power demand profiles proportional to the nominal power demand of the bus. Some examples of power profiles are plotted in Figure 4.

The entire analysis presented in this chapter, and similar approaches proposed in the literature, require that Assumption 1 is verified, i.e., that power demands at the different buses are uncorrelated. Figure 5 shows the covariance matrix computed on the bus active power injections, and shows how correlation is in fact present. This fact was also observed in [25], and is mostly due to the fact that different households follow similar hourly patterns, and are exposed to the same weather conditions. On the other hand, the right panel of Figure 5 shows that the mutual correlation vanishes at high frequencies (shorter time scales). Once measurement are pre-processed through a high-pass filter, it is therefore reasonable to assume uncorrelation. This recommendation is clearly valid not only for the approach proposed in this chapter, but for the other similar approaches reviewed in the literature as well.

In Figure 6, we compute the concentration matrix K in order to verify the sparsity pattern predicted in Theorem 1, and thus apply the centralized identification algorithm proposed in Section 3. The left panel shows how the concentration matrix presents many spurious elements, due to nonlinearity, non-uniform X/R ratio of the lines, non-uniform P/Q ratio, and correlation between power demands. Further numerical experiments confirmed that this latter cause is predominant. The right panel, obtained by performing the same analysis, on the same test grid, but with synthetic uncorrelated power demands, show that the sign patter predicted in Theorem 1 emerges correctly in this case.

Interestingly, the identification algorithm proposed in Section 3, based on the construction of a minimum spanning tree, is quite robust also in the presence of spurious elements in the sample

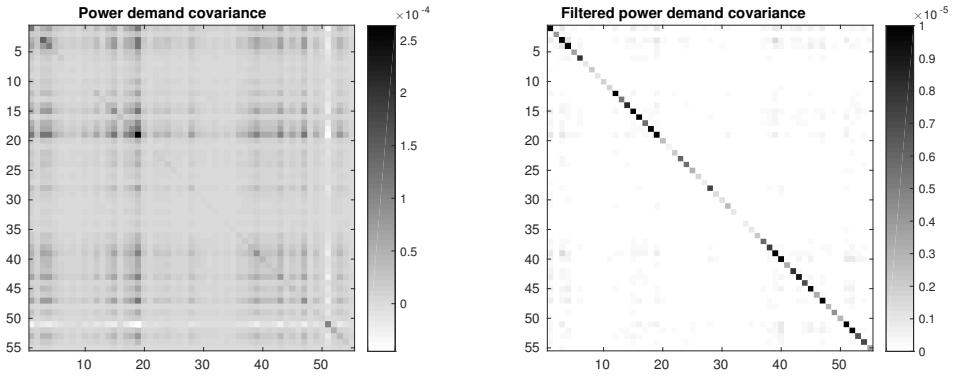

Figure 5: Sample covariance matrix obtained from a 12-hour dataset of real data. The left panel represents the covariance matrix obtained from the raw data, and exhibits relevant inter-bus correlation. The right panel show the covariance matrix obtained after a high pass filter has been applied (stop band frequency: $\frac{1}{8\text{min}}$, pass band frequency $\frac{1}{0.8\text{min}}$). Above this cut-out frequency, power demands are practically uncorrelated.

concentration matrix. Figure 7 shows the result of a typical execution of the algorithm (which in general depends on the specific samples that are measured). The grid topology is reconstructed almost correctly, with the exception of two edges, highlighted in the right panel.

Finally, we consider the distributed statistical hypothesis testing proposed in Section 4. We consider the triad $\mathcal{T} = \{6, 7, 10\}$. Figure 8 shows the concentration matrices K, computed for increasing number of samples and different sets of measurements. On the matrices, we overlay (as black dots) the result of the identification algorithm proposed in Section 4. With as few as 30 samples, the sign pattern predicted by Theorem 2 emerges correctly, and allows the correct reconstruction of the relative position of the three nodes. As the number of samples increases, the concentration matrices become identical.

To illustrate the performance of this distributed approach, in Figure 9 we considered six different triads, and for each one of them we plotted the error rate in the reconstruction of the relative position of the three nodes, for increasing number of samples. For some triads, the error rate decreases extremely fast, and very few samples are needed in order to successfully identify the topology of the triad. In few other cases, slightly more samples are needed.

A natural question, which we have not addressed in this chapter, is about the optimal placement of the sensors (i.e., selection of the triad) in order to maximize the efficiency of the algorithm in selecting the right hypotheses between those available (for example, which bus voltage to measure in order to determine the position of the switches in Figure 3).

6 Conclusions

In this chapter we presented an analysis of the correlation of voltage magnitude measurements in a radial distribution feeder, showing how, under some Assumptions, such correlation encodes information about the topology of the grid.

An immediate application of this result consists in a centralized algorithm for the identification of the topology of the grid. The applicability of this algorithm, and of many other similar algorithms in the literature, is limited by the fact that all voltage buses need to be measured, and many samples are required in order to converge to the correct topology.

In most cases, the identification of the full topology is not even needed. Most topology identification problems can be cast in the form of an hypothesis test: which network switch is closed, which node is closer to the substation, etc. In order to address this need, a distributed statistical test has been proposed. Based on the voltage measurements of a set of only three nodes, it is possible to conclude, after very few samples, on the relative position and interconnection of these nodes. The resulting algorithm is very robust with respect to weakly correlated power demands,

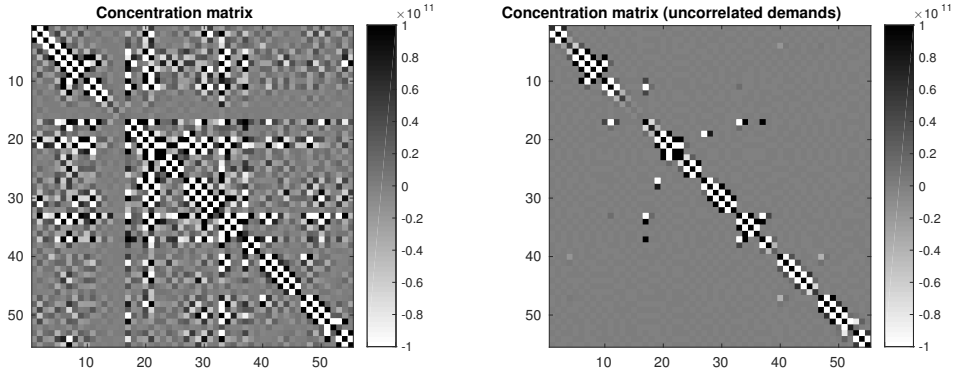

Figure 6: The left panel represents the sample concentration matrix obtained from the real data measurements. The concentration matrix should exhibit the same sparsity pattern of the squared Laplacian. Spurious elements are mainly caused by the correlation between power demands, as shown in the right panel, where the same matrix is computed based on synthetic uncorrelated power demands, and the sparsity patter is practically exact.

and extremely lightweight to implement.

The optimal placement of these triads of sensors, given a specific topology hypothesis to test, is an open problem with relevant practical implications.

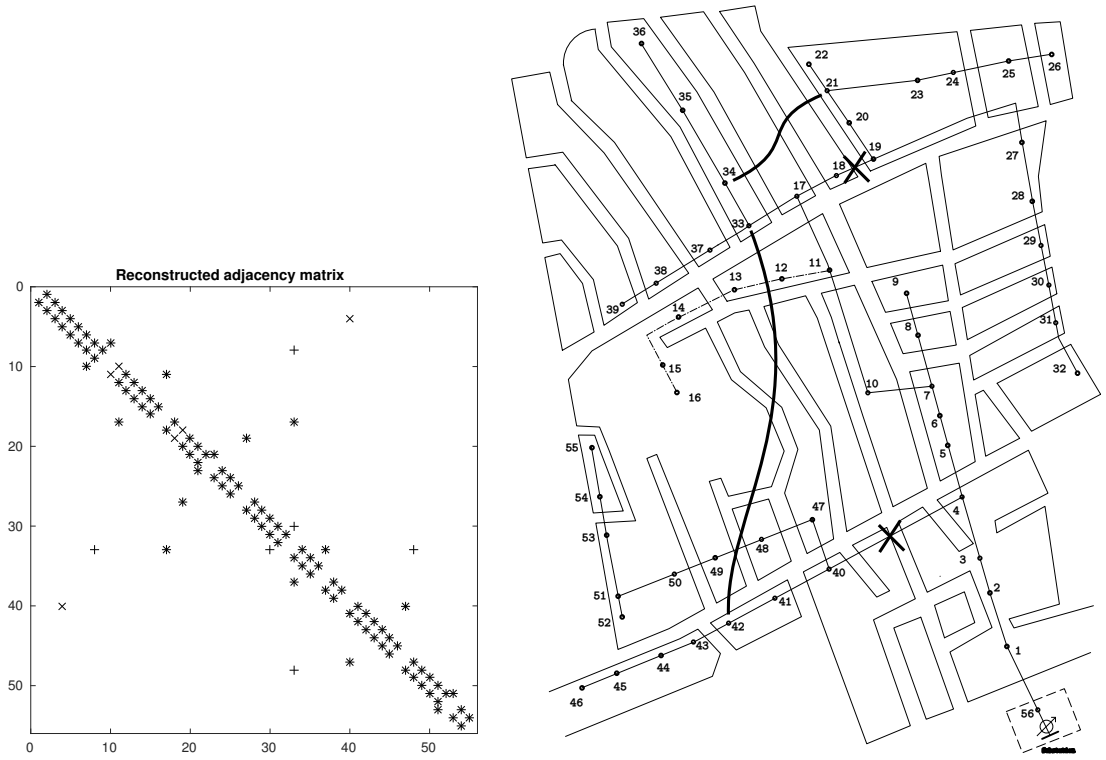

Figure 7: Typical results of the application of the approach presented in Section 3 to the modified IEEE 123 test case, with real power measurement data. The left panel shows how the true Laplacian ($\times$) is correctly identified ($+$) except for two mis-identified edges (highlighted also in the map).

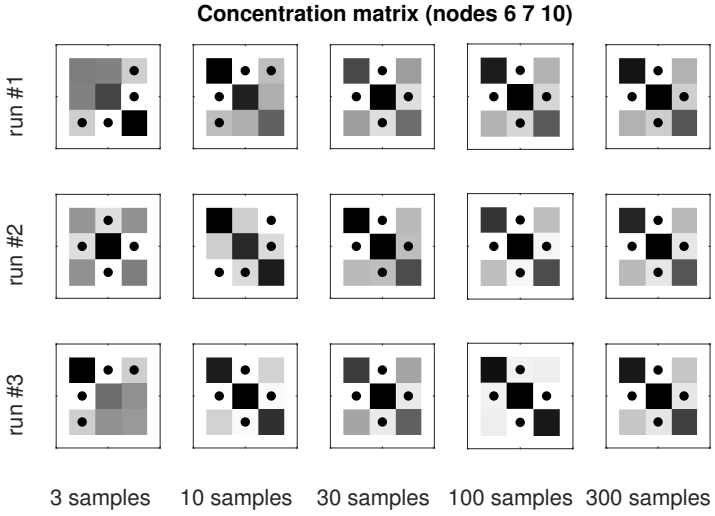

Figure 8: Sample concentration matrix for the voltage measurements collected at three nodes (6, 7, 10). Each column corresponds to a different number of samples. Each row corresponds to a different dataset (corresponding to different starting times during the day). The black dots correspond to the topology identified via the minimum-spanning-tree algorithm. As the number of samples increases, the sample concentration matrix converges to its true value (allowing the identification of the correct topology). For very small sample sets, different realization can yield different results.

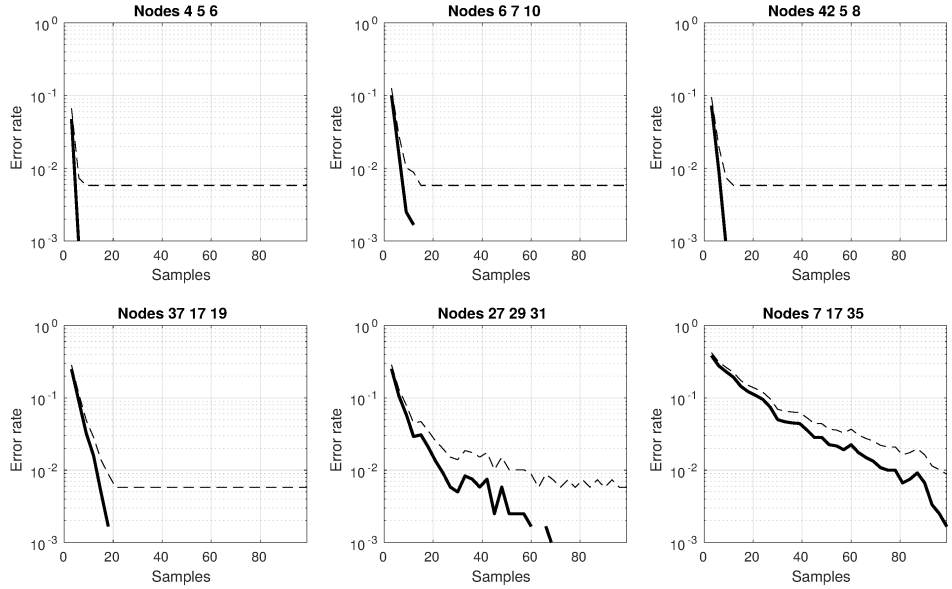

Figure 9: Error rate of the proposed hypothesis-testing algorithm for the identification of the relative connection of different triads of nodes. The thick line represents the unbiased estimate of the error rate computed on 1200 realizations. The dashed line is the 95% confidence interval computed via the Wilson score interval [29], and settles at 0.58% when no errors are observed in the 1200 realizations.

References

[1] Zhou Q, Bialek JW. Generation curtailment to manage voltage constraints in distribution networks. IET Generation, Transmission and Distribution. 2007;1(3):492–498.

[2] Clement-Nyns K, Haesen E, Driesen JLJ. The impact of charging plug-in hybrid electric vehicles on a residential distribution grid. IEEE Transactions on Power Systems. 2010 Feb;25(1):371–380.

[3] Lopes JAP, Soares FJ, Almeida PMR. Integration of electric vehicles in the electric power system. Proceedings of the IEEE. 2011 Jan;99(1):168–183.

[4] ADDRESS. Active Distribution networks with full integration of Demand and distributed energy RESourceS (EU FP7-ENERGY project); 2008. Available from: `http://www.addressfp7.org`.

[5] DREAM. Distributed Renewable resources Exploitation in electric grids through Advanced heterarchical Management (EU FP7-ENERGY project); 2013. Available from: `http://www.dream-smartgrid.eu`.

[6] EvolvDSO. Development of methodologies and tools for new and evolving DSO roles for efficient DRES integration in distribution networks (EU FP7-ENERGY project); 2013. Available from: `http://www.evolvdso.eu`.

[7] PlanGridEV. Distribution grid planning and operational principles for EV mass roll-out while enabling DER integration (EU FP7-ENERGY project); 2013. Available from: `http://www.plangridev.eu`.

[8] Wainwright MJ, Jordan MI. Graphical models, exponential families, and variational inference. Foundations and Trends in Machine Learning. 2008;1(1-2):1–305.

[9] Sharon Y, Annaswamy AM, Motto AL, Chakraborty A. Topology identification in distribution network with limited measurements. In: IEEE Innovative Smart Grid Tech. Conf. (ISGT); 2012. .

[10] Luan W, Peng J, Maras M, Lo J, Harapnuk B. Smart Meter Data Analytics for Distribution Network Connectivity Verification. IEEE Transactions on Smart Grid. 2015 Jul;6(4):1964–1971.

[11] Cavraro G, Arghandeh R, Poolla K, von Meier A. Data-driven approach for distribution network topology detection. In: Proc. IEEE PES General Meeting; 2015. .

[12] He M, Zhang J. A dependency graph approach for fault detection and localization towards secure smart grid. IEEE Transactions on Smart Grid. 2011 Jun;2(2):342–351.

[13] Bolognani S, Bof N, Michelotti D, Muraro R, Schenato L. Identification of power distribution network topology via voltage correlation analysis. In: Proc. IEEE 52nd Annual Conference on Decision and Control (CDC); 2013. .

[14] Weng Y, Liao Y, Rajagopal R. Distributed Energy Resources Topology Identification via Graphical Modeling. IEEE Transactions on Power Systems. 2016;.

[15] Deka D, Backhaus S, Chertkov M. Structure Learning and Statistical Estimation in Distribution Networks - Part I. arXiv:150104131v2 [mathOC]. 2015;.

[16] Deka D, Backhaus S, Chertkov M. Estimating distribution grid topologies: A graphical learning based approach. In: Proc. Power Systems Computation Conference (PSCC); 2016. .

[17] Deka D, Backhaus S, Chertkov M. Learning topology of distribution grids using only terminal node measurements. In: Proc. IEEE International Conference on Smart Grid Communications (SmartGridComm); 2016. .

[18] Liao Y, Weng Y, Liu G, Rajagopal R. Urban Distribution Grid Topology Estimation via Group Lasso. arXiv:161101845v1 [statML]. 2016;.

[19] Weckx S, D'Hulst R, Driesen J. Voltage Sensitivity Analysis of a Laboratory Distribution Grid With Incomplete Data. IEEE Transactions on Smart Grid. 2015 May;6(3):1271–1280.

[20] Bolognani S, Zampieri S. On the existence and linear approximation of the power flow solution in power distribution networks. IEEE Transactions on Power Systems. 2016;31(1):163–172.

[21] Bolognani S, Dörfler F. Fast power system analysis via implicit linearization of the power flow manifold. In: Proc. 53rd Annual Allerton Conference on Communication, Control, and Computing; 2015. .

[22] Cheriton D, Tarjan RE. Finding minimum spanning trees. SIAM Journal on Computing. 1976;5(4):724–742.

[23] Chow CK, Liu CN. Approximating discrete probability distributions with dependence trees. IEEE Transactions on Information Theory. 1968;14(3):462–467.

[24] Yuan M, Lin Y. Model selection and estimation in the Gaussian graphical model. Biometrika. 2007;94(1):19–35.

[25] Pedersen R, Sloth C, Andresen GB, Wisniewski R. DiSC: A Simulation Framework for Distribution System Voltage Control. In: Proc. European Control Conference; 2015. .

[26] Pohl A, Johnson J, Sena S, Broderick R, Quiroz J. High-resolution residential feeder load characterization and variability modelling. In: Proc. 40th IEEE Photovoltaic Specialist Conference (PVSC); 2014. .

[27] Bolognani S. approx-pf - Approximate linear solution of power flow equations in power distribution networks; 2014. GitHub. Available from: `http://github.com/saveriob/approx-pf`.

[28] Kersting WH. Radial distribution test feeders. In: IEEE Power Engineering Society Winter Meeting. vol. 2; 2001. p. 908–912.

[29] Hogg RV, Tanis EA. Probability and statistical inference. 6th ed. Upper Saddle River, NJ: Prentice Hall; 2001.